Published in Hydrogeology Journal 23, issue 4, 619-629, 2015
which should be used for any reference to this work

Can shallow open-loop hydrothermal well-doublets help remediate seawater intrusion?

François De Keuleneer · Philippe Renard

Abstract Recharge through injection wells is a well-established technique to remediate and protect coastal aquifers from saltwater intrusion. In this study, it is shown that hydrothermal doublet installations can also be used to protect coastal aquifers while producing heat or cold for air conditioning. Such a method could be extremely valuable for situations where there is both a need for freshwater and energy production in coastal regions. The efficiency of the proposed approach is tested using Strack's analytical solution on a wide range of scenarios where the number of injection and pumping wells vary as well as the distance between these wells and the coast. The efficiency is evaluated through four control parameters: the relative freshwater volume, the maximum penetration distance of the saltwater toe, the thermal breakthrough time, and the percentage of injected water recycled. The analysis of these parameters computed for 343 scenarios confirms the efficiency of the method. Those results are extremely encouraging even if they still need to be confirmed through field experiments.

Keywords Salt-water/fresh-water relations · Coastal aquifers · Groundwater protection · Open-loop · Hydrothermal well-doublets

Introduction

Freshwater and energy are two essentials for human existence. Freshwater availability is threatened by various sources of pollution. As the world's population living on the coast is constantly growing (Parry et al. 2007), the pressure on coastal aquifers and energy demands in these locations is increasing.

While seawater intrusion is a natural phenomenon, its impact is worsened by intensive freshwater withdrawal (Werner et al. 2013). This problem has attracted the attention of scientists for decades. The saltwater/freshwater interface and the way to characterize it have been studied through a wide variety of methods and models (Bear et al. 1999; Werner et al. 2013). Different approaches to counter or prevent saltwater intrusion have also been developed such as subsurface physical barriers (Bear et al. 1999), recharge wells (Luyun et al. 2011), pumping of brackish water (Mahesha 1996), withdrawal of freshwater through skimming wells and horizontal wells to reduce the upconing of seawater (Saeed et al. 2002), freshwater extraction–injection doublets (Lu et al. 2013), etc. Various optimization methods have also been used in coastal aquifer management to define sustainable groundwater management schemes and to protect pumping wells from saltwater intrusion (Cheng et al. 2000; Mantoglou 2003; Abarca et al. 2006; Koussis et al. 2010; Singh 2014).

Even though the best remediation method appears to be the injection of freshwater (treated wastewater, surface freshwater, desalinized water, etc.) near the saltwater toe to create a hydraulic barrier (Werner et al. 2013), the water needed is not always available. Lu et al. (2013) proved the concept of injection–extraction well pairs to be efficient to counter the saltwater intrusion by re-injecting part of the freshwater extracted. However, the economic costs of such a remediation can be a limiting factor.

Meanwhile, the energy needs for heating and cooling, and the price of fossil fuels, do not stop rising. In 2010, heating and cooling were responsible for 47 % of the European Union's energy consumption (Sparber and Pezzuto 2013). Several alternative and renewable energies have been developed. In that context, open-loop hydrothermal well-doublets using shallow groundwater coupled with heat pumps (Omer 2008) can be very efficient in many locations and domains such as: family houses, administrative buildings, industries, or hotel complexes (Sanner et al. 2003; Lemale and Gourmez 2008; Banks 2009). In coastal regions, the need for cooling is especially high in tourist areas where at the same time freshwater resources are critical.

F. De Keuleneer (✉) · P. Renard
University of Neuchâtel, Centre of Hydrogeology and Geothermics, Rue Emile-Argand 11, 2000, Neuchâtel, Switzerland
e-mail: dekeuleneerf@gmail.com
Tel.: +32472525278

P. Renard
e-mail: philippe.renard@unine.ch

So far, to the knowledge of the authors, no study has yet considered the possibility of using a hydrothermal well-doublet to provide simultaneously a counter measure to seawater intrusion in coastal regions while offering a method of heating or cooling. The present study aims at investigating the feasibility of such a system. Could a combination of several extraction and injection wells be used to produce freshwater and be a source of energy in coastal aquifers while protecting the resource and being economically viable? If yes, this concept could provide an attractive additional value to an otherwise expensive remediation method.

To test the proposed concept, the study is based on the analytical model of seawater intrusion assuming a sharp interface developed by Strack (1976) for confined and unconfined aquifers. While more recent and advanced analytical solutions, as well as numerical models, are available (e.g. Koussis et al. 2012), it is deemed sufficient to test the proposed concept in the simplest configuration first, which is the aim of this paper.

The paper is organized as follows. First, the conceptual model and calculation methods are described. Various scenarios of pumping-injection wells are tested against four control parameters: the relative freshwater volume, the saltwater-toe maximum penetration distance, the thermal breakthrough time and the fraction recycled. The results obtained using those calculation methods are then presented and discussed.

Conceptual model

The conceptual model used in this work is the one proposed by Strack (1976). It assumes a homogeneous, isotropic and semi-infinite coastal aquifer bounded on the side by an infinite and straight coastline. The problem is treated in two dimensions by neglecting vertical flow. Several additional approximations are made such as the Dupuit-Forcheimer assumption involving vertical equipotentials due to a pressure field considered hydrostatic. The lower boundary is an impervious horizontal stratum and the upper boundary is the free water table. The base of the aquifer is assumed to be an impervious horizontal stratum in both cases. It is also assumed that the seawater intrusion can be modeled using a sharp interface. As the saltwater flow velocity is very small compared to that for freshwater, it is neglected. The flow regime is assumed to be in steady state and all the wells are fully penetrating the aquifer; a regional lateral recharge flux is prescribed on the upstream boundary (Strack 1976).

Under those assumptions, the hydraulic head in the domain can be obtained from Strack's potential equations which will be described later. The position of the saltwater/freshwater interface is given using the Ghyben-Herzberg relationship. Figure 1a shows that the aquifer is divided into two areas: the unconfined flow area (zone 2) and the unconfined-interface flow area (zone 1). In zone 2, the freshwater flows across the whole aquifer thickness, and in zone 1, it flows only above the sharp interface separating the fresh and saltwater. The two flow areas are governed by two different equations. In zone 1, the flow thickness is influenced both by the depth of the saltwater/freshwater interface and by the piezometric level, whereas in zone 2, the thickness is only influenced by the piezometric level. Fluxes and groundwater heads have to be continuous at the transition between the two zones. When groundwater is pumped, the limit between the two zones moves inland (Fig. 1b). The counter-measure which is studied in this paper consists of setting up a shallow hydrothermal well-doublet(s) with a heat pump as illustrated conceptually in Fig. 1c. Several configurations with more than two wells will be compared and studied in the following section.

Calculation methods

Flow equations

The solution to the general potential equation proposed by Strack (1976) in the case of n pumping wells is:

$$\Phi(x,y) = \frac{qx}{K} + \sum_{i=1}^{n} \frac{Q_i}{4\pi K} \ln\left[\frac{(x-x_i)^2 + (y-y_i)^2}{(x+x_i)^2 + (y-y_i)^2}\right] \quad (1)$$

where Φ [m^2] is the potential, q [m^2/d] is the upstream regional recharge rate, x [m] is the coordinate of any point in the domain (distance from the coast), y [m] is the coordinate parallel to the coast (the origin is an arbitrary point along the coast), K [m/d] represents the hydraulic conductivity, Q_i [m^3/d] represents the discharge rate of the ith well (it is positive if extracting and negative if injecting) and x_i and y_i are its coordinates.

The hydraulic head h [m] can then be computed for the unconfined case using two equations depending on the zone:

$$\text{Zone 1}: \quad h = \sqrt{\frac{2\Phi\Delta s}{1+\Delta s}} \quad (2)$$

$$\text{Zone 2}: \quad h = -d + \sqrt{2\Phi + (1+\Delta s)d^2} \quad (3)$$

where d [m] is the depth of the impervious substratum below sea level and $\Delta s = \frac{\rho_s - \rho_f}{\rho_f}$ is the dimensionless relative difference between saltwater and freshwater density, with ρ_f and ρ_s being respectively the density of the freshwater and saltwater. Finally, using Ghyben-Herzberg and assuming a density of saltwater and freshwater of respectively 1.025 and 1, the depth of the interface h_s [m] can be deduced from the value of the hydraulic head in zone 1 with:

$$h_s = -40\ h \quad (4)$$

Simulation domain and aquifer parameters

The equations presented in the previous section are valid for a semi-infinite aquifer; however, to test the performance of the

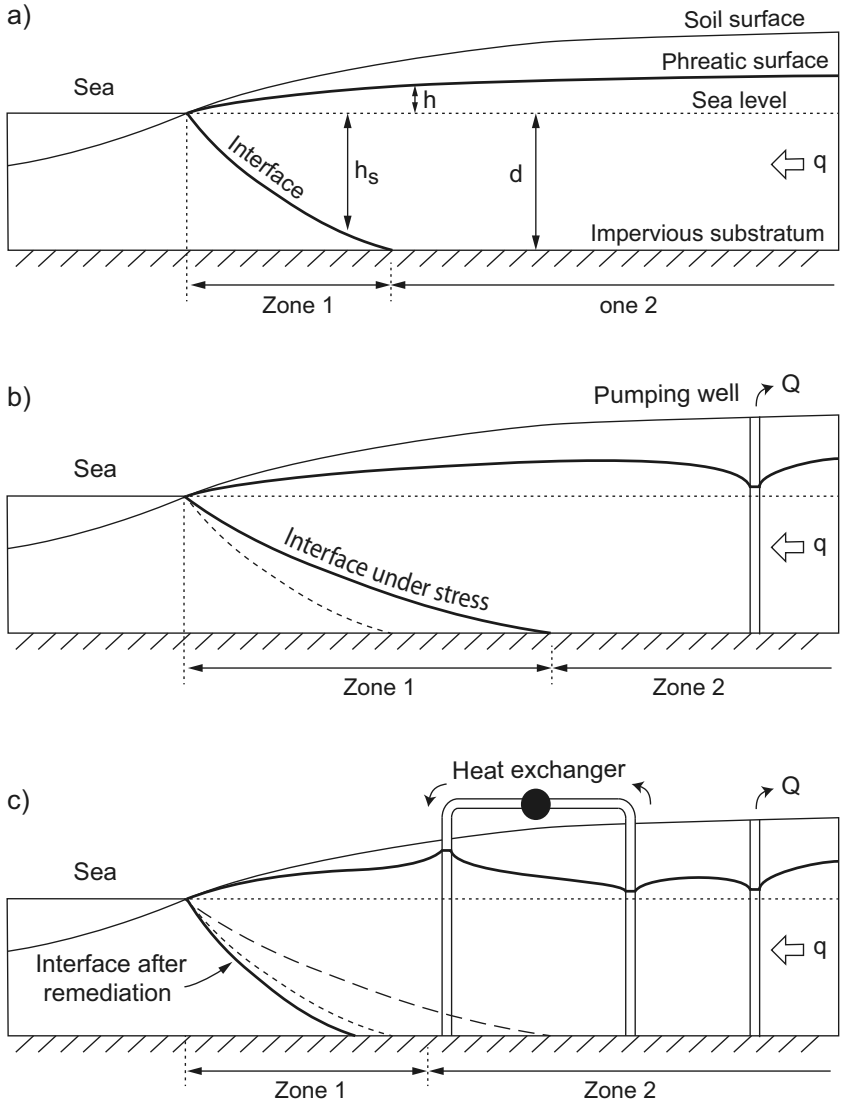

Fig. 1 Schematic 2D vertical sections through the aquifer in the unconfined case: **a** in natural state; **b** under pumping conditions; **c** under pumping conditions and using the proposed open-loop hydrothermal well-doublet(s) system

proposed system, a region of interest of 3 × 3 km is defined. The hydraulic head and position of the interface are computed using Eqs. (1)–(4) with a resolution of 2 m within this domain using MATLAB, which allows visualization of the flow field (Fig. 2a) and the estimation of some parameters such as the maximum depth of penetration of the seawater wedge (see next section). Furthermore, to improve the accuracy of the estimation of the thermal breakthrough time and of the recycled portion of injected water, a refined grid with a dimension of 1.4 × 1.4 km (Fig. 2b) is used in the area surrounding the pumping and injection wells. In this subdomain, a resolution of 1 m is used.

The values of the aquifer parameters were taken from Cheng et al. (2000). The hydraulic conductivity K=100 m/d corresponds to a well-sorted sand or a mixed sand-gravel aquifer (Fetter 2001). The lateral regional recharge is set to q=0.6 m^2/d. No recharge from the top of the aquifer is considered. The depth of the aquifer under sea-level (d) is equal to 14 m.

Evaluation criteria

In the following, the aim is to describe the four criteria used to compare the performances of different configurations of injection and pumping wells and to test the feasibility of the proposed system.

Maximum penetration distance of the saltwater toe (D_{max})

The maximum penetration distances $D_{\max}$ [m] are computed for each scenario by identifying the distances to the coast where the saltwater/freshwater interface meets the impervious substratum of the aquifer. $D_{\max}$ is estimated by computing numerically the heads and depths of the interface using Eqs. (1) to (4) on the regular grid in the 3×3 km region. The resulting values are used to define the position of the toe of the seawater wedge and to estimate the maximum penetration $D_{\max}$ (Fig. 2). As this parameter is calculated using a 2 × 2 m discretization, $D_{\max}$ has an

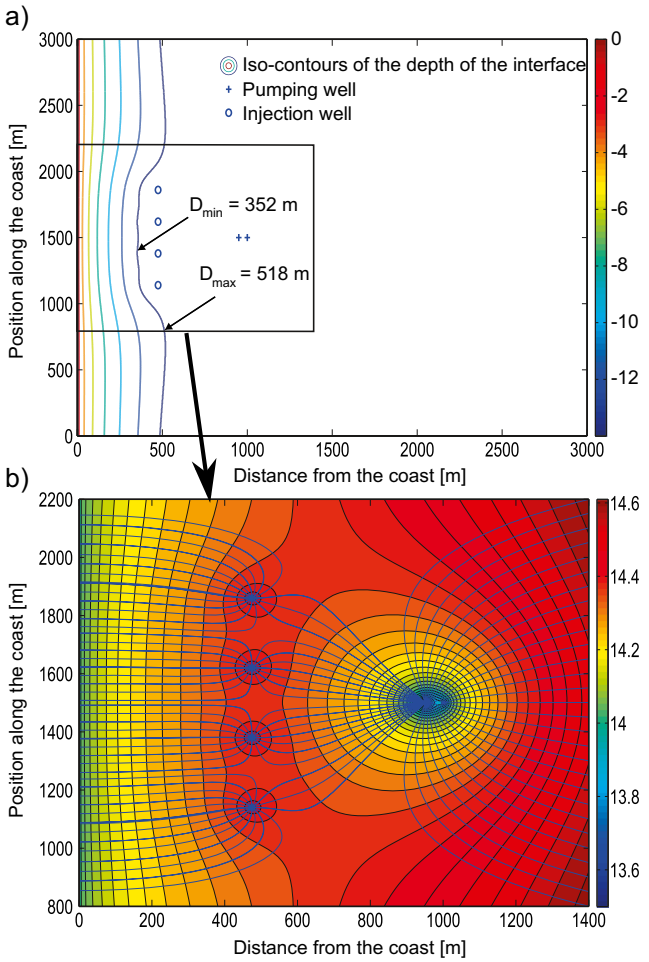

Fig. 2 Illustration of the calculations in the case of the optimized scenario 1 with four injection wells and two pumping wells. D_{min} and D_{max} being respectively the minimum and maximum penetration distance of the saltwater toe in the aquifer. Both maps represent a 2D plan view of the unconfined aquifer: **a** contours showing the depth of the saltwater wedge in the 3 × 3 km region; **b** hydraulic heads and flow lines in the 1.4×1.4 km sub-region. The *color bars* are in meters

accuracy of ±1 m. This accuracy can be enhanced easily by using sub gridding in the region of interest.

Relative volume of freshwater (V_{fresh})

The relative volume of freshwater is the proportion of freshwater in the aquifer. It is defined as the ratio between the total volume of freshwater and the total groundwater volume (fresh+brackish). The volumes are estimated by using the height of the water column obtained by adding the water level (Eqs. 2 and 3) to the depth of the interface (Eq. 4) calculated on the regular grid in the 3×3 km region. This water column height is multiplied by the area of the grid cells. For the total groundwater volume, the water column heights above the impervious substratum (h+d) are taken into account throughout the whole aquifer area. For the freshwater volume, the computation is different for zone 1 where only the water column height
above the interface is considered (h+h_s), whereas, in zone 2, all the water column heights above the substratum are computed. The precision of this calculation can be enhanced if necessary by increasing the discretization.

Hydraulic and thermal breakthrough time (respectively T_{hyd} and T_{th})

The hydraulic breakthrough time is evaluated by considering the shortest pathway followed by a water particle leaving the injection well(s) to the pumping well(s). To determine this pathway, 25 particles are placed around each injection well. The particle paths are then computed by tracking the particle position and following the groundwater head gradients. These calculations are carried out on the 1.4×1.4 km grid with a resolution of 1 m. A small time step dt is imposed to ensure that the particle trajectory is sufficiently accurate. In particular, the maximum distance travelled at each time step is set to 1 m.

Among all the particles leaving the injection well(s), only the one heading to the pumping wells are kept. The fastest of these latter particles follows the shortest path and its hydraulic breakthrough time is given by summing all the time steps dt multiplied by the porosity n. The accuracy of this method has been controlled by comparing the results of the numerical calculation with analytical expressions available for simple doublet configuration. Here the numerical solution was necessary since the number and location of the wells could prevent the use of a simple analytical formula. Finally, following Milnes and Perrochet (2013), the thermal breakthrough time is computed by multiplying the hydraulic breakthrough time by a retardation factor R:

$$R = 1 + \frac{(1-n)}{n}\frac{\mathrm{Cp_s}}{\mathrm{Cp_l}} \quad [-] \tag{5}$$

where n, $\mathrm{Cp_s}$ and $\mathrm{Cp_l}$ are respectively the porosity (0.3 [−]) and the volumetric heat capacity of the solid (2.2×10^6 J/m^3/K) and the liquid (4.2×10^6 J/m^3/K).

This method allows computing of the earliest breakthrough time. However, when considering complex scenarios such as the one shown in Fig. 2, one realizes that only a small portion of the recycled water will reach the pumping well at this breakthrough time. Therefore, using these breakthrough times to estimate the longevity of a system places the designer on the safe side.

Portion recycled of injected water (Rec)

To compute the proportion of injected water recycled in the pumping well, the x component of the Darcy velocity must be integrated between two stagnation points located on a line parallel to the coast (Milnes and Perrochet 2013).

$$\mathrm{Rec}(l) = d\frac{\int_{s1}^{s2} K\frac{dh}{dx}(l)}{Q\mathrm{tot}}dy \tag{6}$$

where, Rec [−] is the recycled percentage of injected water, d [m] is the depth of the substratum under the seawater level, Qtot [m^3/d] is the total discharge rate

Table 1 Air temperature statistics for Rome for the period 1961–1990 (Desiato et al. 2005; World Meteorological Organization 2014)

	Jan	Feb	Mar	Apr	May	Jun	Jul	Aug	Sep	Oct	Nov	Dec
Mean temperature	8.3	9.05	10.5	13.1	17.0	20.6	23.4	23.6	20.9	17	12.7	9.5
Min. daily temperature	3.7	4.4	5.8	8.3	11.9	15.6	18.2	18.4	15.8	12.0	8.1	5.1
Max. daily temperature	12.9	13.7	15.3	18.0	22.0	25.6	28.6	28.7	26.0	22.0	17.2	13.9

injected, $s1$ [m] and $s2$ [m] are the y location of the two stagnation points and $\frac{dh}{dx}$ [−] is the derivative of the hydraulic head in the x direction. The two stagnation points are identified automatically by mapping the locations where the hydraulic gradient is close to zero. The integration is then carried out numerically.

Hydrothermal discharge rate calculation

The second part of the evaluation consists of testing the feasibility of the proposed system in terms of energy production. For this purpose, it is necessary to relate the total discharge rate that needs to be extracted from the aquifer with the energy demand.

In this paper, it was decided to assume that the hydrothermal open-loop wells could be used by a tourist resort along the Mediterranean coastline. Next, to make a reasonable estimation of the energy demand for such a resort, the monthly consumption for heating provided by a hotel in Rome (Italy) was used. The peak load (month with the highest heat need) is used to constrain the design of the system. For the sake of simplicity, the discharge rate of the installation will be assumed constant in the following calculations. The peak consumption is then divided by the number of hours contained in a month to obtain the mean power P_{mean} the heat pump (HP) has to produce. This power is linked to the difference in temperature between the heating temperature (20–21 °C) and the mean temperature of the month. The maximum power P_{max} [kW] is evaluated as follows:

$$P_{\text{max}} = P_{\text{mean}} \times \frac{(T_{\text{i}} - T_{\text{minext}})}{(T_{\text{i}} - T_{\text{meanext}})} \tag{7}$$

where P_{mean} is the mean power to be furnished during the coolest month, T_{i} is the indoor temperature needed and T_{minext} and T_{meanext} are respectively the minimum and mean exterior temperature.

The following equation is then used to evaluate the discharge rate of the hydrothermal installation Q_{geoth} [m^3/h] (Lemale and Gourmez 2008):

$$Q_{\text{geoth}} = \frac{P_{\text{max}} \times \left(1 - \frac{1}{\text{COP}}\right)}{1.16 \times \Delta T} \tag{8}$$

where ΔT is the temperature variation between the pumped and the injected water, COP is the HP's performance coefficient and 1.16 is the heat capacity of water per unit of volume in kWh/m^3/K. The discharge rate, being in cubic meters per hours, is multiplied by 24 hours per day (h/d) to obtain cubic meters per day. Nevertheless, the HP mean power may also be used to calculate the mean discharge rate and the peak demands would be satisfied by a higher discharge rate during those peaks (Lemale and Gourmez 2008).

The air temperatures for Rome are presented in Table 1. The mean temperatures correspond to the mean between the minimum daily temperatures and the maximum daily temperatures. This may differ slightly from the real mean monthly temperatures in Rome but it will only have a minor impact on the evaluation of the feasibility of the proposed system.

The peak demand is in December and rises to 231,445 kWh. The mean power (P_{mean} in [kW]) the HP has to furnish is found dividing the peak demand by the hours contained in a month:

$$P_{\text{mean}} = \frac{231445}{720} = 321.45 \tag{9}$$

and the maximum power (P_{max} in [kW]) of the HP is found using data of Table 1 in Eq. (7) with T_{i}=20 °C:

$$P_{\text{max}} = 321.45 \times \frac{(20 - 5.1)}{(20 - 9.5)} = 456.15 \tag{10}$$

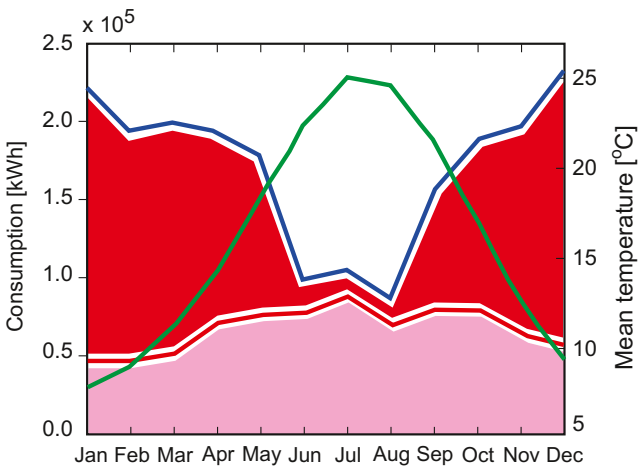

Fig. 3 Plot of the mean temperature (*green line*) and the total heat consumption (*blue line*). The two colored zones represent the needs for domestic water (*pink area*) and for space heating and pool heating (*red area*)

Table 2 Number of pumping and injection wells for the different configurations tested in the numerical experiments

Configuration	No. of pumping wells	No. of injection wells
1	1	1
2	2	2
3	3	3
4	4	4
5	1	2
6	1	3
7	1	4

The hydrothermal discharge rate (Q_{geoth} in [m^3/d]) is then evaluated using Eq. (8) with a COP of 3.8 and a ΔT of 5.5 °C:

$$Q_{\text{geoth}} = \frac{456.15 \times \left(1 - \frac{1}{3.8}\right)}{1.16 \times 5.5} \times 24 = 1266.8 \qquad (11)$$

The discharge rate has been approximated to 1,260 m^3/d to simplify the calculations.

Now, looking at the power the heat pump has to furnish throughout the year in Fig. 3, one realizes that the maximum power is only needed during the two coolest months. When comparing these observations to Table 1, one sees that during the summer months, the heat production is nearly all dedicated to domestic hot water. Having a reversible heat pump, the constant discharge rate of the installation can produce a great amount of cold during the hotter months, enhancing the economic benefit of the installation.

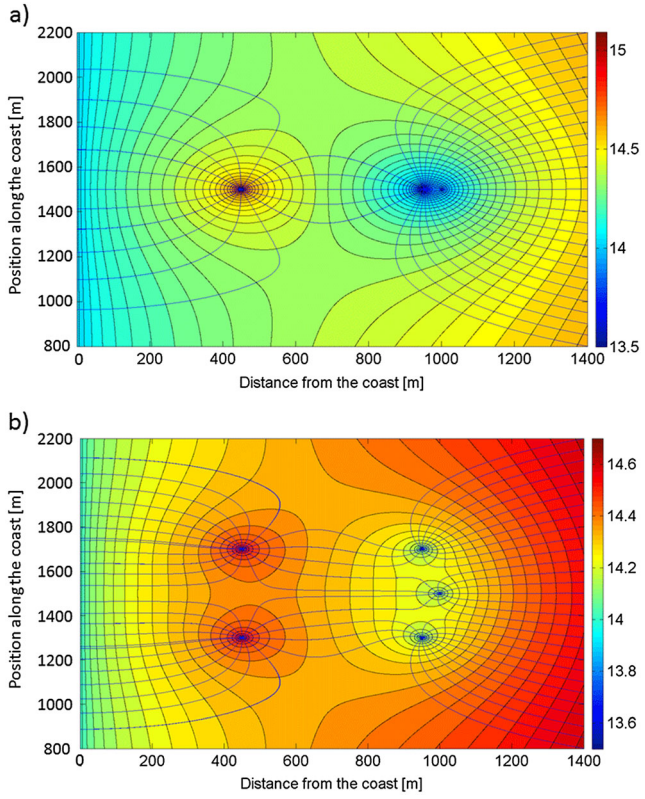

Fig. 4 Example of flow fields computed for two of the seven well configurations tested: **a** configuration 1, one doublet with the pumping and injection wells respectively located at (*1000,1500*) and (*450,1500*), **b** configuration 2, two doublets with pumping wells located at (*950,1300*) and (*950,1700*) and the injection wells at (*450,1300*) and (*450,1700*)

Scenarios

To determine the most efficient dispositions of wells, 343 different combinations were tested. Seven different configurations are considered (Table 2). Each configuration corresponds to a given number of injection and pumping wells. All configurations include, in addition to the wells described in Table 2, a pumping well located at coordinates (1000, 1500) and used for the freshwater needs of the presumed hotel. Two of the configurations are illustrated in Fig. 4.

For each configuration, 49 scenarios were computed. The scenarios correspond to different locations of the injection wells (distance to the coast varying between 350 and 500 m with a step of 25 m) and pumping wells (distance to the coast varying between 800 and 950 m with steps of 25 m). The y coordinates of the well locations are constant within a configuration. They vary depending on the number of wells in the pumping or injection line: for one well, y=1500; for two wells y_1=1300 and y_2=1700; for three wells y_1=1200, y_2=1500 and y_3=1800 and for four wells y_1=1140, y_2=1380, y_3=1620 and y_4=1860.

The global discharge rate pumped and injected for the hydrothermal installation remains constant at 1,260 m^3/d and is equally divided between the pumping and injection wells. Varying the number of pumping wells with a fixed number of injection wells did not give interesting results and is, therefore, not presented in the paper.

Systematic analysis and optimization

To find the optimal scenarios, the fact that the calculations are rapid and rather simple enables a crude method to be applied, consisting of scanning systematically the parameter space and evaluating the criteria for each scenario. The results are presented through a step-by-step approach and allow plotting and analyzing the Pareto front. All scenarios leading to saltwater reaching the pumping wells are not retained. Indeed, Strack's equations are not valid for these cases and those scenarios are not interesting from a practical perspective.

Step by step approach

The method consists of analyzing first the volume and distance parameters obtained by the calculations conducted on the 3 × 3 km domain. The latter domain is used to ensure that the maximum penetration distance is obtained and that the relative freshwater volume includes the whole region to minimize artefacts.

Table 3 Number of selected scenarios according to the various control parameters and for the different configurations

	Configuration						
	1	2	3	4	5	6	7
Top 20 %: relative freshwater volume	0	0	4	9	0	9	17
Lower 20 %: maximum penetration distance	0	0	0	2	1	14	15
Top 30 %: thermal breakthrough time	0	0	1	6	0	0	0
Lower 20 %: proportion of injected water recycled	0	0	4	9	0	1	3
Total for each configuration	0	0	9	26	1	24	35

For each control parameter, the difference between the maximum and the minimum is considered and is named the interval.

The first step consists of selecting the scenarios corresponding to the best protection of the aquifer in terms of the highest freshwater volume V_{fresh} as this is considered to be the most important parameter at a global scale. The resulting scenarios are then ranked in terms of maximum penetration distance of the saltwater toe. For the volume parameter, only the scenarios belonging in the higher 20 % of the interval are kept. Similarly, concerning the distance parameter, only the scenarios present in the lower 20 % are kept. Once the optimal scenarios regarding these 2 parameters are identified, the thermal breakthrough time and the recycled-portion parameters are calculated for these scenarios using the 1.4×1.4 km sub-region. The scenarios having both a high T_{th} and a low Rec are retained as the optimal ones.

Results

To test the efficiency of the method, three different situations are compared: the natural state, the stressed state due to withdrawal of freshwater and, finally, the remediated states resulting from the various scenarios.

Table 4 Number of selected scenarios (according to the control parameters) obtained when varying the distance (in meters) between the coast and the line of pumping wells

	Distance: pumping line to the coast						
	950	925	900	875	850	825	800
Top 20 %: relative freshwater volume	19	13	5	2	0	0	0
Lower 20 %: maximum penetration distance	5	5	4	4	5	5	4
Top 30 %: thermal breakthrough time	4	2	1	0	0	0	0
Lower 20 %: proportion of recycled water	10	5	1	1	0	0	0
Sum for each distance	38	25	11	7	5	5	4

Table 5 Number of selected scenarios (according to the control parameters) obtained when varying the distance (in meters) between the coast and the line of injection wells

	Distance: injection line to the coast						
	350	375	400	425	450	475	500
Top 20 %: relative freshwater volume	0	0	5	9	9	8	8
Lower 20 %: maximum penetration distance	0	0	0	0	2	13	17
Top 30 %: thermal breakthrough time	0	0	3	3	1	0	0
Lower 20 %: proportion of injected water recycled	0	0	6	7	3	1	0
Sum for each distance	0	0	14	19	15	22	25

Saltwater wedge in natural and stressed states

In a natural state, the aquifer presents a saltwater wedge. The saltwater toe reaches 420 m inland (D_{max}) and the relative freshwater volume is R_{fresh}=95.567 %. Adding a net withdrawal of 450 m^3/d at 1,000 m from the coast in the middle of the aquifer (y=1,500 m) makes the saltwater toe move inland (D_{max}=576 m) and makes the freshwater volume diminish (R_{fresh}=94.703 %).

Results produced by the various scenarios

Out of the 343 scenarios tested, 180 were not retained. Indeed, the configurations and well locations in these scenarios lead the saltwater to reach the pumping well(s). Table 3 presents an overview of the results. For each control parameter, the numbers of scenarios belonging to the best cases (higher or lower intervals depending on the criteria) are reported. Looking at the total number of

Table 6 List of all optimum scenarios regarding the volume and distance parameters based on the 3×3 km model. L_{pump} is the distance between the coast and the pumping well(s) of the doublet(s) (in meters), L_{inj} is the distance between the coast and the injection well(s) (in meters), V_{fresh} is the relative freshwater volume (in percent of the total water volume) and D_{max} the maximum penetration distance of the saltwater toe from the coastline (in meters)

Scenario	Configuration	$L_{\text{pump (m)}}$	$L_{\text{inj (m)}}$	V_{fresh}	D_{max}
1	7	950	475	95.222	518
2	7	925	475	95.205	518
3	7	900	475	95.188	518
4	6	950	500	95.201	516
5	7	950	500	95.214	510
6	6	925	500	95.183	516
7	7	925	500	95.196	510
8	7	900	500	95.178	510

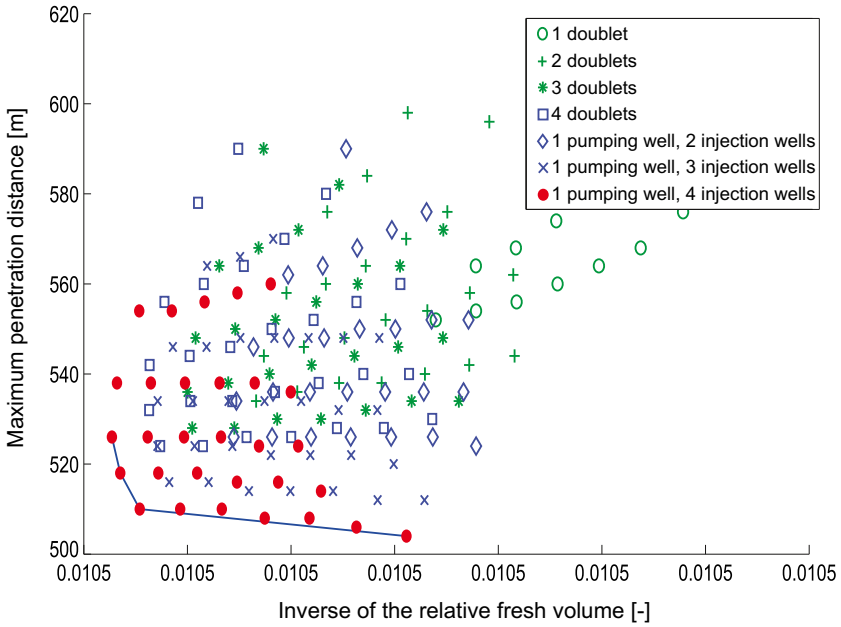

Fig. 5 Scatter plot of the maximum penetration distance (D_{max}) as a function of the inverse of the relative freshwater volume (V_{fresh}) for the various scenarios. The optimal location is the *lower left corner*

scenarios selected in the higher or lower intervals for each configuration in Table 3, configurations 4, 6 and 7 are found to be the most efficient. Indeed, having less than three injection wells does not produce an efficient hydraulic barrier as the saltwater tends to flow around these wells.

In Table 4, the number of selected scenarios are compared with respect to the distance between the coast and the line of pumping wells. It is found that the best scenarios (for almost all criteria) correspond to the largest distances (950 or 925 m) as expected. The only criterion that does not show any trend in this table is the maximal penetration distance D_{max} because it is influenced mainly by the distance between the injection wells and the coast.

Finally, in Table 5, the numbers of selected scenarios are compared with respect to the distance between the coast and the line of injection wells. A first striking observation is that the scenarios with the line of injection wells at less than 400 m are never selected and should therefore not be considered. The number of scenarios selected according to the maximum penetration distance D_{max} increases when moving the injection line inland; however, this criterion cannot be taken alone, since the other criteria worsen at large distances to the coast. T_{th} and Rec show optimal values when the injection is placed from 400 to 450 m. The closer the injection line is to the pumping wells, the smaller is the breakthrough time and the higher is the proportion recycled.

Table 7 Thermal breakthrough time and recycled portion of injected water computed on the 1.4×1.4 km area for the selected scenarios

Scenario	Thermal breakthrough time [d]	Portion recycled of injected water [%]
1	13,020	31.42
2	11,778	32.74
3	10,586	34.10
4	9,684	34.34
5	11,550	33.21
6	8,657	35.73
7	10,409	34.56
8	9,314	35.97

Selecting the best compromises

Step by step optimization

The first step consists of keeping only the scenarios producing a V_{fresh} in the higher 20 % of the interval. Among these scenarios, the ones with a D_{max} in the lower 20 % of the interval are kept. The retained scenarios are listed in Table 6.

More generally, Fig. 5 shows how D_{max} correlates with $1/V_{fresh}$ for the different scenarios. An important characteristic of this figure is the existence of a Pareto front. Above the front, all the scenarios are not optimal in the sense that one can find another scenario in which either D_{max} is smaller or V_{fresh} is larger. Below, along the Pareto front, one has to accept a compromise: an improvement in terms of D_{max} implies to worsen V_{fresh}. The best possible scenarios are those along the Pareto front.

Comparing the results obtained for V_{fresh} and D_{max} in Tables 3, 4, 5, and 6 and Fig. 5, one observes that they all converge toward the same conclusion: the best results are given by configuration 7 even if configuration 6 also offers close results.

For each scenario listed in Table 6, T_{th} and Rec are calculated in the 1.4×1.4 km focus area. Table 7 regroups the results given by these two parameters. One finds then that scenarios 1 and 2 offer the best results. As they are very close in configurations and distances, only scenario 1

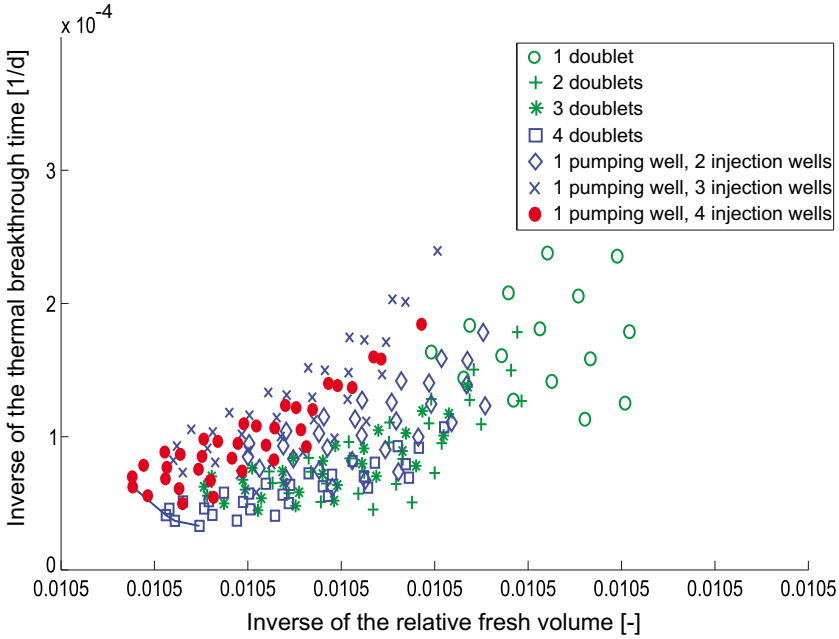

Fig. 6 Scatter plot of the inverse of the thermal breakthrough time (T_{th}) versus the inverse of the relative freshwater volume (V_{fresh})

will be discussed further.Note that if T_{th} must be increased for the sustainability of a specific project, one should consider configuration 4 as indicated by Fig 6, but this will imply a reduction of V_{fresh} as compared to scenario 1.

The comparison of scenario 1 with the natural and stressed states shows that it permits improvement of the situation: V_{fresh} is 95.222 % which is 0.52 % higher than V_{fresh} in the stressed state and is 0.35 % lower than the natural state; the maximum saltwater toe penetration is 58 m shorter compared to the stressed state but still 98 m greater than in the natural state. T_{th} reaches 13,020 days (35 years) and Rec=31.42 %. These results are also satisfying knowing that the thermal breakthrough time T_{th} corresponds to the fastest particles among the 31.42 % of recycled water. The recycled portion indicates also that only a part of the injected freshwater will be lost to the sea. Figure 2 illustrates the flow field and position of the saltwater wedge toe.

The same procedure was applied for the confined aquifer situation using the corresponding analytical solution (Strack 1976) and lead to similar conclusions. In this case, the optimal scenarios were obtained from both configurations 4 and 7. The decision of choosing between these two configurations can be based on a rough evaluation of the costs. The results of such a calculation using only the drilling costs and a given pump price is provided in Table 8 and shows that configuration 7 appears to be 47.6 % cheaper than configuration 4. For a real project, additional cost estimates including all the installation costs (hydrothermal installation, connecting pipes) and running costs (energy) would have to be carried out to be able to compare accurately the different scenarios.

Discussion

A new framework is proposed in which a remediation method to counter saltwater intrusions in coastal aquifers is combined with hydrothermal use of the groundwater. The example discussed in this paper shows that such a system could be efficient for an unconfined aquifer. Comparing the three different states (natural, stressed, and remediated), the deterioration following the freshwater withdrawal is partly remediated by the implementation of the open-loop hydrothermal well-doublets that act as an efficient hydraulic barrier. Numerical experiments were also made in the case of a confined aquifer and the results are similar. The only significant difference was the value of the breakthrough time; it is smaller for a confined aquifer because the same volume of water flows through a thinner section.

It is noted that, even if the setup is slightly different, the optimal distance between the injection wells and the coast resulting from the present study are close to the optimal injection location obtained in the experimental and numerical study of Luyun et al. (2011). In both cases, the injection is more effective when located close to the

Table 8 Rough evaluation of the cost for each scenario. The cost per meter of drilling is fixed at 300 USD for a 7-inch (18-cm) borehole and the price of each pump is 10,000 USD

Configuration	1	2	3	4	5	6	7
Costs [USD]	30,200	47,400	64,600	81,800	34,400	38,600	42,800

saltwater toe. Furthermore, when comparing the results of this work to the ones obtained by Lu et al. (2013), again similar general conclusions are obtained: the saltwater toe penetration is repelled after implementation of injection wells. However, this approach is different because it uses the reinjected groundwater to produce energy, and because the search for the best configuration is carried out with a constant discharge rate and other types of control parameters. The aim here is not to enhance the withdrawal but to remediate a deterioration of the freshwater resource.

In general, one should not forget that this study is based on important assumptions and that the methods present several limitations. The results are based on an analytical model (Strack 1976) assuming homogeneity and neglecting the dispersion of the salt along the interface in 3D. Strack's solution assumes, in addition, the coast to be infinite and a horizontal base for the aquifer. All these assumptions could be relaxed by using more sophisticated models. For example, image wells and the principle of superposition could be used to account for boundaries (Mantoglou 2003). Aquifers with an inclined base could also be considered (Koussis et al. 2012). Density dependent flow or complex geometries could be treated using numerical models. Numerical models would also allow investigation of some more efficient configurations such as the use of skimming wells or horizontal wells (Saeed et al. 2002). In practice, a numerical model would certainly be required to design the best configuration for a given site. The model would include the real geometry of the aquifer, probably multiple freshwater withdrawals, vertical recharge from the precipitation, seasonal variations, spatial heterogeneities, variation in temperatures at the pumping and injection wells (Milnes and Perrochet 2013), and so on.

However, ultimately, the proof that the principle described in this paper is working should be obtained by conducting a real field experiment. This was not feasible for the present study, but all the calculations done so far indicate that hydrothermal doublets have a good chance of helping in the remediation of coastal aquifers suffering from seawater intrusion while producing an important amount of sustainable heat and cold. Moreover, the energy and cost savings induced by the geothermal installation make this method economically viable.

Conclusion

The research described in this paper is based on the Strack (1976) analytical solutions for groundwater flow in a coastal aquifer assuming a sharp interface with seawater. The results show that using open-loop hydrothermal well-doublets could be an efficient way to remediate seawater intrusion. Various configurations and distances between wells have been considered. The optimal scenarios in the realistic example case that was studied here include four injection wells and produce the most efficient hydraulic barrier. A clear improvement regarding the distance of penetration and the relative volume of freshwater is obtained as compared to a state without the use of the well-doublet. The thermal breakthrough time is estimated to be larger than 30 years, which satisfies the conditions for a hydrothermal installation to be sustainable. Such results are extremely encouraging; however, further investigations should be carried out to confirm that the proposed method would be really effective for a given site, especially because of the unavoidable assumptions related to the use of an analytical solution in this study.

Acknowledgements The authors are thankful to Pierre Perrochet, Jaouher Kerrou, and Vincent Badoux for all their help, discussions and comments throughout this study. The authors are thankful to Paul Taylor for reviewing the language.

References

Abarca E, Vazquez-Sune E, Carrera J, Capino B, Gamez D, Batlle F (2006) Optimal design of measures to correct seawater intrusion. Water Resour Res 42. doi:10.1029/2005wr004524

Banks D (2009) Thermogeological assessment of open-loop well-doublet schemes: a review and synthesis of analytical approaches. Hydrogeol J 17:1149–1155. doi:10.1007/s10040-008-0427-6

Bear J, A H-DC, Sorek S, Ouazar D, Herrera I (1999) Seawater intrusion in coastal aquifers: concepts, methods and practices. Kluwer, Dordrecht, The Netherlands

Cheng AHD, Halhal D, Naji A, Ouazar D (2000) Pumping optimization in saltwater-intruded coastal aquifers. Water Resour Res 36:2155–2165

Desiato F, Lena F, Baffo F, Suatoni B, Toreti A (2005) Indicatori del CLIMA in Italia [Indicators of CLIMA in Italy]. APAT, Agenzia per la Protezione dell'Ambiente e per i Servici Tecnici, Rome

Fetter CW (2001) Applied hydrogeology, 4th edn. Prentice Hall, Upper Saddle River, NJ

Koussis AD, Georgopoulou E, Kotronarou A, Lalas DP, Restrepo P, Destouni G, Prieto C, Rodriguez JJ, Rodriguez-Mirasol J, Cordero T, Gomez-Gotor A (2010) Cost-efficient management of coastal aquifers via recharge with treated wastewater and desalination of brackish groundwater: general framework. Hydrol Sci J 55:1217–1233. doi:10.1080/02626667.2010.512467

Koussis AD, Mazi K, Destouni G (2012) Analytical single-potential, sharp-interface solutions for regional seawater intrusion in sloping unconfined coastal aquifers, with pumping and recharge. J Hydrol 416:1–11. doi:10.1016/j.jhydrol.2011.11.012

Lemale JG, Gourmez D (2008) Guide technique Les pompes à chaleur géothermique sur aquifère [Technical guidelines: geothermal groundwater heat pumps]. BRGM, Orléans, France

Lu CH, Werner AD, Simmons CT, Robinson NI, Luo J (2013) Maximizing net extraction using an injection–extraction well pair in a coastal aquifer. Ground Water 51:219–228. doi:10.1111/j.1745-6584.2012.00973.x

Luyun R, Momii K, Nakagawa K (2011) Effects of recharge wells and flow barriers on seawater intrusion. Ground Water 49:239–249. doi:10.1111/j.1745-6584.2010.00719.x

Mahesha A (1996) Control of seawater intrusion through injection–extraction well system. J Irrig Drain Eng 122:314–317. doi:10.1061/(asce)0733-9437(1996)122:5(314)

Mantoglou A (2003) Pumping management of coastal aquifers using analytical models of saltwater intrusion. Water Resour Res 39

Milnes E, Perrochet P (2013) Assessing the impact of thermal feedback and recycling in open-loop groundwater heat pump

(GWHP) systems: a complementary design tool. Hydrogeol J 21:505–514. doi:10.1007/s10040-012-0902-y

Omer AM (2008) Ground-source heat pumps systems and applications. Renew Sustain Energy Rev 12:344–371. doi:10.1016/j.rser.2006.10.003

Parry MLC, OF, Palutikof JP, van der Linden PJ, Hanson CE (2007) Contribution of Working Group II to the Fourth Assessment Report of the Intergovernmental Panel on Climate Change, 2007. Cambridge University Press, Cambridge

Saeed MM, Bruen M, Asghar MN (2002) A review of modeling approaches to simulate saline-upconing under skimming wells. Nord Hydrol 33:165–188

Sanner B, Mands E, Sauer MK (2003) Larger geothermal heat pump plants in the central region of Germany. Geothermics 32:589–602. doi:10.1016/j.geothermics.2003.07.010

Singh A (2014) Optimization modelling for seawater intrusion management. J Hydrol 508:43–52. doi:10.1016/j.jhydrol.2013.10.042

Sparber W, Pezzuto S (2013) Hybrid systems and heat pumps. 4th European Conference on Renewable Heating and Cooling RHC-Platform, Dublin, Ireland, 22–23 April 2013

Strack ODL (1976) Single-potential solution for regional interface problems in coastal aquifers. Water Resour Res 12:1165–1174. doi:10.1029/WR012i006p01165

Werner AD, Bakker M, Post VEA, Vandenbohede A, Lu CH, Ataie-Ashtiani B, Simmons CT, Barry DA (2013) Seawater intrusion processes, investigation and management: recent advances and future challenges. Adv Water Resour 51:3–26. doi:10.1016/j.advwatres.2012.03.004

World Meteorological Organization (2014) http://www.wmo.int/pages/index_en.html. Accessed Dec 2014